

ALTITUDE AND FLIGHT SPEED CONTROL SYSTEM ON VTOL-PLANE UAVS USING THE LQR METHOD

AHMAD ASHARI* AND ANDI DHARMAWAN

Department of Computer Science and Electronics
Universitas Gadjah Mada

Sekip Utara, BLS 21 Yogyakarta 55281, Indonesia

*Corresponding author: ashari@ugm.ac.id; andi_dharmawan@ugm.ac.id

Received May 2021; accepted August 2021

ABSTRACT. *A VTOL-Plane UAV has a wide flight speed range. Rotary wings can only fly at very low horizontal translation speeds. Fixed-wing requires a more incredible speed than the stall speed to get enough wing lift. Combined fixed-wing and rotary-wing concepts can fly at speeds below the stall speed. The flight speed determines the amount of wing lift and elevon torque that affects the altitude and attitude of the vehicle. Therefore, the UAV requires robust altitude and flight speed control. The altitude and flight speed control system on the VTOL-Plane UAV is designed to apply the LQR method to finding the full-state feedback gain value. The UAV model simulation is performed to test the results of the control method. Direct testing is carried out on VTOL-Plane flight by converting control output variables into a PWM to regulate brushless motor rotational speed and servos angles to adjust surfaces.*

Keywords: VTOL-Plane UAV, LQR, Full state, Feedback, PWM, Robust

1. **Introduction.** Unmanned Aerial Vehicle (UAV) has become common in the military and civilian world in recent years [1]. Military missions using conventional aircraft are currently high cost and have low maneuverability [2]. By implementing UAV, costs can be reduced. Besides, with its small size, the UAV can maneuver an area quickly [3]. However, a UAV still has problems such as integration into the flight base, reliability, and flight safety [4].

Fixed-wing UAVs fly fast and for long periods but require a runway for take-off and landing [5]. A rotary-wing UAV, on the other hand, is not energy efficient [6]. Therefore, it was not suitable for missions requiring high endurance. However, it has the uncanny ability to levitate, as well as take-off and land vertically. Therefore, it can operate almost anywhere without having to search for open spaces [7].

The VTOL-Plane UAV has two independent propulsion systems for hover and level flight [8]. Combining the two concepts of fixed-wing and rotary-wing, a VTOL-Plane UAV has the advantages of both systems and eliminates their disadvantages [9]. Thus, a UAV VTOL-Plane has vertical take-off and landing capability and has a high flight speed and longer endurance than a rotary-wing [10]. A VTOL-Plane can carry out close surveillance missions in static flying conditions with its VTOL and hover capabilities. This capability does not belong to a fixed-wing UAV that needs to continue moving in the air [11].

The development of a VTOL-Plane controller focuses on two aspects: the design of the flight attitude controller and the design of the flight path controller [12]. The attitude control design deals with the VTOL-Plane response in maintaining stability. VTOL-Plane has three flight modes: fixed-wing, hybrid, and rotary-wing mode [13]. In fixed-wing mode, the UAV must fly at high speed [14], whereas in rotary-wing mode, the UAV can only fly

at low speeds. The development of the hybrid mode ensures the UAV can fly at medium speed by activating all actuators.

We need a control method to maintain the altitude and speed of the VTOL-Plane, so it can still retain its flying attitude when maneuvering [15,16]. Linear Quadratic Regulator (LQR) is a control method most widely used in aviation because LQR is a control method with good performance and durability and can optimize control [17].

The LQR control method uses some states as feedback in controlling the attitude and velocity of flying. The feedback states consist of angular rotational movement, altitude, flight speed, and their changes with time [14]. They are measured by using an Inertial Measurement Unit (IMU) sensor and a barometer. The sensor readings are then processed by the LQR control algorithm and used to adjust the attitude and speed of flight. The results of this study aim that the UAV can maintain its speed while simultaneously controlling its altitude autonomously using the Linear Quadratic Regulator (LQR).

The rest of the paper is structured as follows: Section 2 addresses the theory and formula, Section 3 describes the experimental setup, Section 4 discusses the experimental results and performance analysis, and finally, Section 5 concludes the paper.

2. Theory and Formula. The VTOL-Plane hybrid UAV has two propulsion systems that work independently, namely the lift and horizontal propulsion. Lifting propulsion is generated by four brushless motors in a vertical direction. The UAV's flying attitude can be controlled by the difference in lifts within the four motors. Besides, the UAV surface control, which is supported by horizontal propulsion, can also play a role in stabilizing the UAV's attitude [18].

When the VTOL-Plane is flying at a speed below stall speed, the wing lift is less than the vehicle's weight. This condition requires the support of the four lifting motors to provide additional lift to prevent the UAV's height from dropping. The rotating speed of the lifting motor will maintain altitude by increasing the lifting force. The flight speed hold control affects the altitude hold control process. Both are very important for implementation in VTOL-Plane hybrid flight.

Before designing the altitude and flight speed control system on the VTOL-Plane UAV, a control system to deal with unwanted rotational motion must be created first. This control is called the stabilizer or countering unwanted rotation control. This control is needed to maintain the UAV level condition, namely when the lifting motors and the wings are horizontal. The system requirements specifications for countering unwanted rotation control need to be met before establishing the altitude and flight speed control system.

The countering unwanted rotation control system on the VTOL-Plane will maintain the UAV's rotational movement, including roll, pitch and yaw motion. The actuators that work on this control system are the four lift and elevon motors located on the wing. The IMU sensor and magnetometer provide input to the system in the current UAV rotation angle. The difference in rotational speed of the lifting motor and lift from the elevon deflection will be adjusted so that the UAV remains in a level condition. The expected rise time for countering unwanted roll and pitch rotation for this research is 1 second. The response time is chosen so that the UAV does not experience disorientation.

After the stabilizer control system can make the UAV fly in level conditions, a control system to adjust the altitude and flying speed can be designed and built. The barometer sensor provides an input of the UAV's height relative to the ground, and the GPS provides information of its flight speed relative to the ground (ground speed). The motor thruster will change its rotating speed to maintain ground speed.

Furthermore, the four lifting motors are used to adjust the flying altitude of the UAV. The rise time for speed and altitude hold is expected to be no more than 2 seconds. Rise time that is too long can cause the UAV to stall because it has lost its lift.

The VTOL-Plane control algorithm consists of several parts, including other procedures, autopilot procedures, and sub-programs that are constantly repeated for the flight commands from GCS. The autopilot procedure will be active if there is an AUTO command from GCS. In the autopilot procedure, the system calculates the angle deviation of the aircraft orientation from the desired setpoint based on the output from the sensor.

The VTOL-Plane mathematical model is designed based on Newton's Laws and Euler's Equation. Equations (1)-(6) show the VTOL-Plane dynamic model. $[u \ v \ w \ p \ q \ r]^T$ is the linear and angular velocity variable about the body axis. $[x \ y \ z \ \phi \ \theta \ \psi]^T$ is a linear and angular position variable regarding the earth's axis. $[F_x \ F_y \ F_z \ \tau_\phi \ \tau_\theta \ \tau_\psi]^T$ is the variable of force and torque. F_p is the horizontal driving motor force [19]. F_T is the total lift for the four vertical motors. F_w is the wing lift. $[F_{w_x} \ F_{w_y} \ F_{w_z}]^T$ is a matrix of forces from the wind on the longitudinal, lateral, and vertical axes. $[\tau_x \ \tau_y \ \tau_z]^T$ is the control torque matrix produced by the difference in the vertical motor rotational speed. $[\tau_{w_x} \ \tau_{w_y} \ \tau_{w_z}]^T$ is the torque from the wind hitting the UAV [20].

$$\dot{p} = \frac{I_{yy} - I_{zz}}{I_{xx}} r q + \frac{\tau_x + \tau_{w_x}}{I_{xx}} \quad (1)$$

$$\dot{q} = \frac{I_{zz} - I_{xx}}{I_{yy}} p r + \frac{\tau_y + \tau_{w_y}}{I_{yy}} \quad (2)$$

$$\dot{r} = \frac{I_{xx} - I_{yy}}{I_{zz}} p q + \frac{\tau_z + \tau_{w_z}}{I_{zz}} \quad (3)$$

$$\dot{u} = r v - q w - g s(\theta) + \frac{F_p + F_{w_x}}{m} \quad (4)$$

$$\dot{v} = p w - r u + g s(\phi) c(\theta) + \frac{F_{w_y}}{m} \quad (5)$$

$$\dot{w} = q u - p v + g c(\phi) c(\theta) + \frac{-F_T - F_{w_z} + F_{w_y}}{m} \quad (6)$$

where m = UAV mass; u = longitudinal velocity; v = lateral velocity; w = vertical velocity; \dot{u} = change in longitudinal angular velocity with time; \dot{v} = change in lateral angular velocity with time; \dot{w} = change in vertical angular velocity with time; p = roll angular velocity; q = pitch angular velocity; r = yaw angular velocity; \dot{p} = change in roll angular velocity with time; \dot{q} = change in pitch angular velocity angle to time; \dot{r} = change in yaw angular velocity to time; F_p = horizontal driving motor force; F_{w_x} = wing lift in longitudinal or x -axis; F_{w_y} = wing lift in lateral or y -axis; F_{w_z} = wing lift in vertical or z -axis; τ_x = control torque around x -axis; τ_y = control torque around y -axis; τ_z = control torque around z -axis; τ_{w_x} = torque from the wind hitting the UAV around x -axis; τ_{w_y} = torque from the wind hitting the UAV around y -axis; τ_{w_z} = torque from the wind hitting the UAV around z -axis; I_{xx} = moment of inertia around the x -axis; I_{yy} = moment of inertia around the y -axis; I_{zz} = moment of inertia around the z -axis.

3. Experimental Setup. The system is designed according to system requirements. The electronic system is one that needs attention. There are three main parts in an electronic system, namely, input, processing, and output. Inertial Measurement Unit (IMU) sensors and Global Positioning System (GPS) sensors provide information. An IMU consists of an accelerometer, gyroscope, and magnetometer sensor. The IMU sensor used is the GY86 series. This sensor consists of the MPU6050 (accelerometer and gyroscope sensor), HMC5883L (magnetometer sensor), and MS5611 (barometer sensor). Figure 1 shows the VTOL-Aircraft that was used in this study.

The Linear Quadratic Regulator (LQR) method was used in this study. The LQR method is used to determine the value of the \mathbf{K} matrix [21]. The \mathbf{K} matrix is the full-state feedback gain of the control system created. Figure 2 shows a block diagram of the

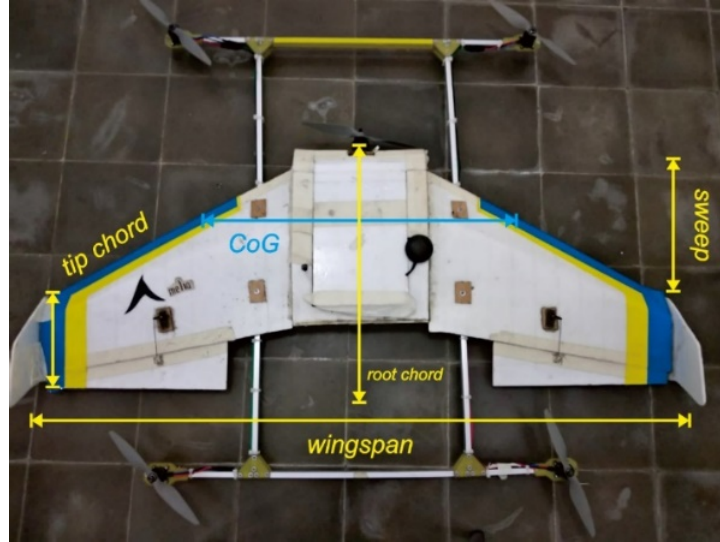


FIGURE 1. UAV VTOL-Plane

VTOL-Plane control system. The control system model is obtained by changing from a dynamic mathematical model to a state-space equation [22]. The VTOL-Plane control system model is obtained by converting Equations (1)-(6) to state-space Equation (7).

$$\begin{bmatrix} \dot{\phi} \\ \dot{\theta} \\ \dot{\psi} \\ \dot{p} \\ \dot{q} \\ \dot{r} \\ \dot{u} \\ \dot{w} \\ \dot{x} \\ \dot{z} \end{bmatrix} = \begin{bmatrix} 0 & 0 & 0 & 1 & 0 & 0 & 0 & 0 & 0 & 0 & 0 \\ 0 & 0 & 0 & 0 & 1 & 0 & 0 & 0 & 0 & 0 & 0 \\ 0 & 0 & 0 & 0 & 0 & 1 & 0 & 0 & 0 & 0 & 0 \\ 0 & 0 & 0 & 0 & \frac{I_{yy} - I_{zz}}{I_{xx}} r & 0 & 0 & 0 & 0 & 0 & 0 \\ 0 & 0 & 0 & 0 & 0 & \frac{I_{zz} - I_{xx}}{I_{yy}} p & 0 & 0 & 0 & 0 & 0 \\ 0 & 0 & 0 & 0 & \frac{I_{xx} - I_{yy}}{I_{zz}} p & 0 & 0 & 0 & 0 & 0 & 0 \\ 0 & 0 & 0 & 0 & 0 & 0 & 0 & 0 & 0 & 0 & 0 \\ 0 & 0 & 0 & 0 & 0 & 0 & 0 & 0 & 0 & 0 & 0 \\ 0 & 0 & 0 & 0 & 0 & 0 & 1 & 0 & 0 & 0 & 0 \\ 0 & 0 & 0 & 0 & 0 & 0 & 0 & 1 & 0 & 0 & 0 \end{bmatrix} \begin{bmatrix} \phi \\ \theta \\ \psi \\ p \\ q \\ r \\ u \\ w \\ x \\ z \end{bmatrix} + \begin{bmatrix} 0 & 0 & 0 & 0 & 0 \\ 0 & 0 & 0 & 0 & 0 \\ 0 & 0 & 0 & 0 & 0 \\ 0 & 0 & \frac{1}{I_{xx}} & 0 & 0 \\ 0 & 0 & 0 & \frac{1}{I_{yy}} & 0 \\ 0 & 0 & 0 & 0 & \frac{1}{I_{zz}} \\ \frac{1}{M} & 0 & 0 & 0 & 0 \\ 0 & \frac{1}{M} & 0 & 0 & 0 \\ 0 & 0 & 0 & 0 & 0 \\ 0 & 0 & 0 & 0 & 0 \end{bmatrix} \begin{bmatrix} u_1 \\ u_2 \\ u_3 \\ u_4 \\ u_5 \end{bmatrix}$$

$$\begin{bmatrix} \phi \\ \theta \\ \psi \\ u \\ z \end{bmatrix} = \begin{bmatrix} 1 & 0 & 0 & 0 & 0 & 0 & 0 & 0 & 0 & 0 \\ 0 & 1 & 0 & 0 & 0 & 0 & 0 & 0 & 0 & 0 \\ 0 & 0 & 1 & 0 & 0 & 0 & 0 & 0 & 0 & 0 \\ 0 & 0 & 0 & 0 & 0 & 0 & 1 & 0 & 0 & 0 \\ 0 & 0 & 0 & 0 & 0 & 0 & 0 & 0 & 0 & 1 \end{bmatrix} \begin{bmatrix} \phi \\ \theta \\ \psi \\ p \\ q \\ r \\ u \\ w \\ x \\ z \end{bmatrix} + \begin{bmatrix} 0 & 0 & 0 & 0 & 0 \\ 0 & 0 & 0 & 0 & 0 \\ 0 & 0 & 0 & 0 & 0 \\ 0 & 0 & 0 & 0 & 0 \\ 0 & 0 & 0 & 0 & 0 \end{bmatrix} \begin{bmatrix} u_1 \\ u_2 \\ u_3 \\ u_4 \\ u_5 \end{bmatrix} \quad (7)$$

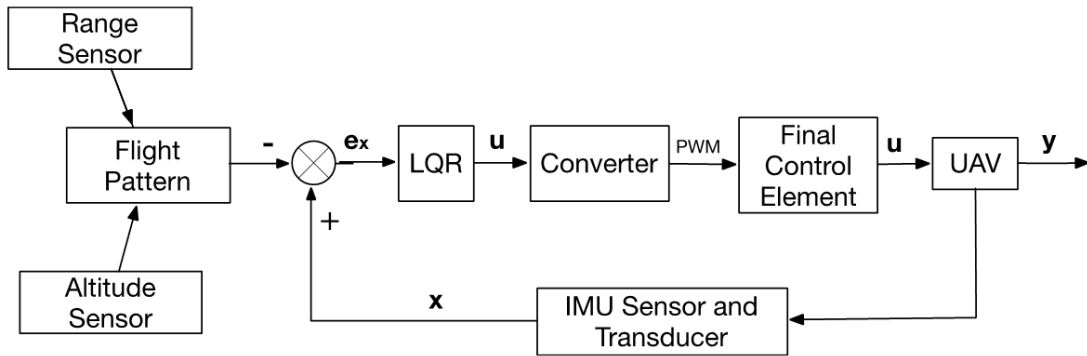


FIGURE 2. Block diagram of the control system

4. Result Discussions. The resulting model is then simulated using the parameters of the UAV in the real world. This simulation is done by automatically tuning the gain \mathbf{Q} of the LQR method [23]. The tuning takes place automatically until it finds the optimal system response by simulation. After the simulation stops and finds the optimal system response, the output of automatic tuning is a full-state feedback gain \mathbf{K} matrix. Automatic tuning consists of 3 steps, namely tuning to adjust the stabilization, altitude, and cruise speed.

Stabilization simulation (also known as countering unwanted rotations) is performed by providing variations in the \mathbf{Q} value for countering unwanted rotations, in the form of Q_ϕ , Q_θ , Q_ψ as \mathbf{Q} angle and Q_p , Q_q , Q_r as \mathbf{Q} angular velocity, automatically. The variation in the \mathbf{Q} value will produce the full-state feedback gain \mathbf{K} , namely $K_{\tau_\phi, \phi}$ and $K_{\tau_\phi, p}$ for countering unwanted roll, $K_{\tau_\theta, \theta}$ and $K_{\tau_\theta, q}$ for countering unwanted pitch, and $K_{\tau_\psi, \psi}$ and $K_{\tau_\psi, r}$ for countering unwanted yaw.

Furthermore, the UAV flight altitude controller (on the z -axis of the earth frame) is also started by tuning the control components Q_z and Q_{v_z} automatically through simulation. The result of tuning the values Q_z and Q_{v_z} were used to maintain the height. The height setpoint used is 10 meters. The altitude control system will be active immediately after the take-off process is complete. UAV altitude control testing is carried out to test the UAV's ability to maintain its position at the setpoint altitude. \mathbf{Q} tuning is done automatically using the simulator with the Riccati equation calculation. The process of tuning the gain \mathbf{Q} yields the gain values $K_{z.F_z}$ and $K_{v_z.F_z}$. The results of auto-tuning the \mathbf{Q} value on the altitude control can be seen in Table 1.

 TABLE 1. Optimal \mathbf{Q} and \mathbf{K} values for altitude control

\mathbf{Q}	\mathbf{K}
$Q_z = 21$	$K_{z.F_z} = 4.58$
$Q_{v_z} = 2$	$K_{v_z.F_z} = 8.18$

Figure 3 shows the simulation and real-world VTOL-Plane altitude control response results, respectively. The initial deviation given on the test is approximately 2 m. The results of the response in the simulation show a rise time of 1.71 seconds to fix the height value to 10 m. In the simulation, there is a deviation of 0.11 m, but it is still below the allowable tolerance (+1 m). The resulting settling time is 3.11 seconds. However, real-world validation has different results compared to the simulation. In real-world validation, the resulting rise time value is 0.8 seconds; the deviation that occurs is 0.94 m, and the resulting settling time is 1.8 seconds. Even though there is a difference from the simulation, the deviation is still below the allowable tolerance. This difference occurs because the simulation does not consider wind conditions, air friction force, and several other environmental parameters. However, because environmental influences are not very influential, the system response is still optimal.

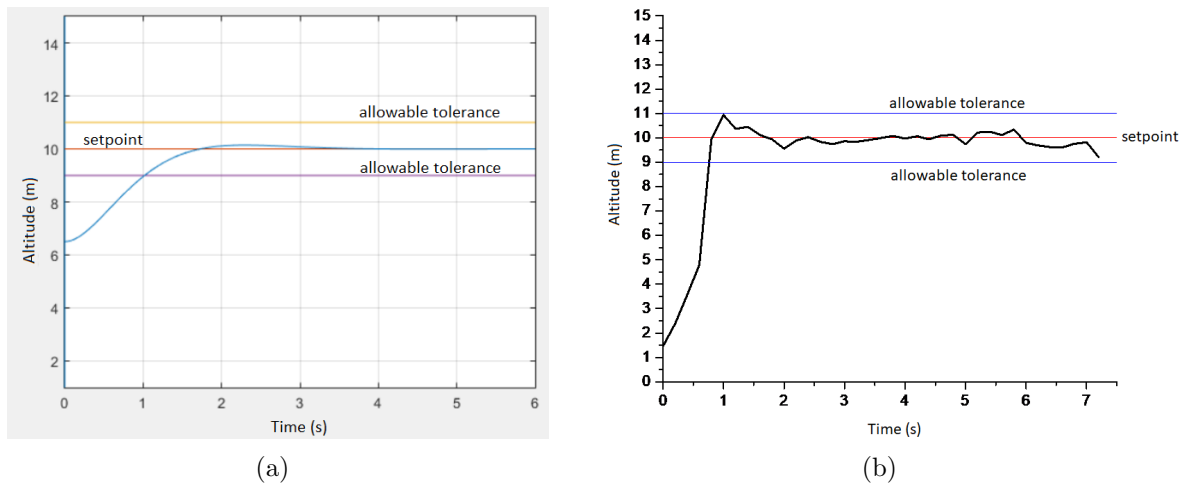


FIGURE 3. Altitude control: (a) Simulation response; (b) validation response

The process of making a UAV speed control system on the x -axis of the earth frame also begins by tuning the control components Q_x and Q_{v_x} . The result of tuning the values of Q_x and Q_{v_x} is used to maintain speed. The speed setpoint used is 6 m/s. The speed control will be active immediately after the take-off process is complete. UAV control testing is carried out to test the UAV's ability to maintain speed after the take-off process. The UAV control testing was carried out for 6 seconds. To get the Q_x and Q_{v_x} values, tuning the \mathbf{Q} value start from 1. Adjusting for the gain \mathbf{Q} is also done automatically using the simulator. The process of tuning the gain \mathbf{Q} yields the gain values $K_{x.F_x}$ and $K_{v_x.F_x}$. The results of auto-tuning the \mathbf{Q} value on the speed control can be seen in Table 2.

TABLE 2. Optimal \mathbf{Q} and \mathbf{K} values for speed control

\mathbf{Q}	\mathbf{K}
$Q_x = 9$	$K_{x.F_x} = 3$
$Q_{v_x} = 0.8$	$K_{v_x.F_x} = 4.09$

Figure 4 shows the results of the VTOL-Plane flight speed control response through real-world simulation and validation sequentially. The initial deviation given on the test is approximately 1.5 m/s. The simulation shows a rise time response of 0.8 seconds, a deviation of 0.18 meters, and a settling time of 3.8 seconds. Besides that, there is no steady-state error. The validation process shows that it shows similar characteristics compared to the simulation. The resulting rise time for real-world validation is 0.97 seconds, the deviation is 0.37 meters, and the settling time is 2 seconds. The real-world validation does not show a steady-state error.

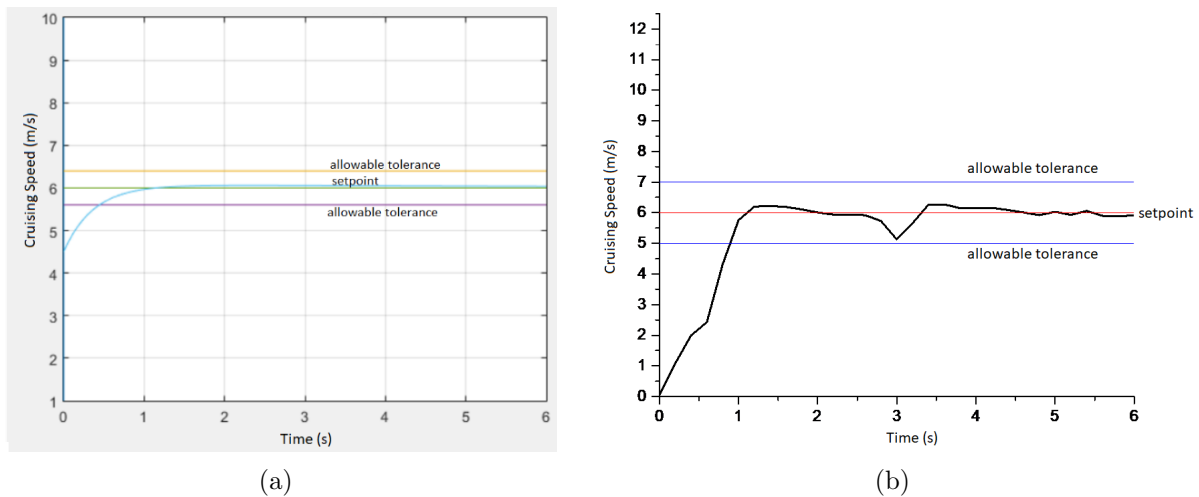


FIGURE 4. Speed control: (a) Simulation response; (b) validation response

5. Conclusions. Controlling the altitude and flight speed of the UAV VTOL-Plane produces a responsive control response. No deviation occurs outside the permitted tolerances. The rise time required by the altitude and speed control system is relatively short, namely 0.3 seconds and 0.4 seconds, respectively. The settling time generated by the height control is 0.7 seconds, and the speed regulator is 1.7 seconds. This response shows that the altitude and speed control on the VTOL-Plane can control the flight well.

However, the GPS-based flight speed control system is still very easily disturbed by airspeed in the test environment. Therefore, it is necessary to have a flight speed control system for the object's velocity relative to the earth equipped with an airspeed sensor as compensation if the airspeed condition in which the VTOL-Plane is flying is high enough. Besides, the application of artificial intelligence is needed to make the control adaptive. Improving the quality of the coefficient measurement on mechanics is also necessary to increase the accuracy of the control calculations.

Acknowledgement. The Ministry of Research and Technology, Republic of Indonesia supported this work under the PTUPT research scheme 2020.

REFERENCES

- [1] A. Ruangwiset, An approach of wing attachment to improve endurance of quadrotor, *2016 2nd Asian Conference on Defence Technology (ACDT)*, pp.89-92, doi: 10.1109/ACDT.2016.7437649, 2016.
- [2] M. Becker and D. Sheffler, Designing a high speed, stealthy, and payload-focused VTOL UAV, *2016 IEEE Systems and Information Engineering Design Symposium (SIEDS)*, pp.176-180, doi: 10.1109/SIEDS.2016.7489294, 2016.
- [3] A. Dharmawan, A. Ashari and A. E. Putra, Quadrotor flight stability system with Routh stability and Lyapunov analysis, *AIP Conference Proceedings*, vol.1755, doi: 10.1063/1.4958609, 2016.
- [4] U. Ozdemir et al., Design of a commercial hybrid VTOL UAV system, *J. Intell. Robot. Syst.*, vol.74, nos.1-2, pp.371-393, doi: 10.1007/s10846-013-9900-0, 2014.
- [5] J. Zhang, Z. Guo and L. Wu, Research on control scheme of vertical take-off and landing fixed-wing UAV, *2017 2nd Asia-Pacific Conference on Intelligent Robot Systems (ACIRS)*, pp.200-204, doi: 10.1109/ACIRS.2017.7986093, 2017.
- [6] T. K. Priyambodo, A. Dharmawan and A. E. Putra, PID self tuning control based on Mamdani fuzzy logic control for quadrotor stabilization, *AIP Conference Proceedings*, vol.1705, doi: 10.1063/1.4940261, 2016.
- [7] J. K. Gunarathna and R. Munasinghe, Development of a quad-rotor fixed-wing hybrid unmanned aerial vehicle, *2018 Moratuwa Engineering Research Conference (MERCon)*, pp.72-77, doi: 10.1109/MERCon.2018.8421941, 2018.
- [8] F. Çakici and M. K. Leblebicyodlu, Control system design of a vertical take-off and landing fixed-wing UAV, *IFAC-PapersOnLine*, vol.49, no.3, pp.267-272, doi: 10.1016/j.ifacol.2016.07.045, 2016.

- [9] A. Lindqvist, E. Fresk and G. Nikolakopoulos, Optimal design and modeling of a tilt wing aircraft, *2015 23rd Mediterr. Conf. Control Autom.*, pp.701-708, doi: 10.1109/MED.2015.7158828, 2015.
- [10] Y. Demitrit, S. Verling, T. Stastny, A. Melzer and R. Siegwart, Model-based wind estimation for a hovering VTOL tailsitter UAV, *2017 IEEE International Conference on Robotics and Automation (ICRA)*, pp.3945-3952, doi: 10.1109/ICRA.2017.7989455, 2017.
- [11] K. Z. Y. Ang et al., Development of an unmanned tail-sitter with reconfigurable wings: U-Lion, *The 11th IEEE International Conference on Control & Automation (ICCA)*, pp.750-755, doi: 10.1109/ICCA.2014.6871015, 2014.
- [12] S. Hou and R. Ling, Tracking control for underactuated VTOL aircraft, *2017 29th Chinese Control and Decision Conference (CCDC)*, pp.1646-1650, doi: 10.1109/CCDC.2017.7978781, 2017.
- [13] D. Orbea, J. Moposita, W. G. Aguilar, M. Paredes, R. P. Reyes and L. Montoya, Vertical take off and landing with fixed rotor, *2017 CHILEAN Conference on Electrical, Electronics Engineering, Information and Communication Technologies (CHILECON)*, pp.1-6, doi: 10.1109/CHILECON.2017.8229691, 2017.
- [14] T. Win, H. T. C. Nyunt and H. M. Tun, Pitch attitude hold autopilot for YTU EC-001 fixed-wing unmanned aerial vehicle, *2019 1st International Symposium on Instrumentation, Control, Artificial Intelligence, and Robotics (ICA-SYMP)*, pp.78-81, doi: 10.1109/ICA-SYMP.2019.8646286, 2019.
- [15] J. Zhang, J. Yan, P. Zhang, D. Yuan and X. Hou, Design and flight stability analysis of the UAV close cooperative formation control laws, *2018 Chinese Control and Decision Conference (CCDC)*, pp.142-147, doi: 10.1109/CCDC.2018.8407120, 2018.
- [16] Z. Zaludin and E. Gires, Automatic flight control requirements for transition flight phases when converting long endurance fixed wing UAV to VTOL aircraft, *2019 IEEE International Conference on Automatic Control and Intelligent Systems (I2CACIS)*, pp.273-278, doi: 10.1109/I2CACIS.2019.8825042, 2019.
- [17] A. Dharmawan, A. Ashari and A. E. Putra, Translation movement stability control of quad tiltrotor using LQR and LQG, *Int. J. Intell. Syst. Appl.*, vol.10, no.3, pp.10-21, doi: 10.5815/ijisa.2018.03.02, 2018.
- [18] H. Gu, X. Lyu, Z. Li, S. Shen and F. Zhang, Development and experimental verification of a hybrid vertical take-off and landing (VTOL) unmanned aerial vehicle (UAV), *2017 International Conference on Unmanned Aircraft Systems (ICUAS)*, doi: 10.1109/ICUAS.2017.7991420, 2017.
- [19] A. Dharmawan, A. E. Putra, I. M. Tresnayana and W. A. Wicaksono, The obstacle avoidance system in a fixed-wing UAV when flying low using LQR method, *2019 International Conference on Computer Engineering, Network, and Intelligent Multimedia (CENIM)*, pp.1-7, doi: 10.1109/CENIM.48368.2019.8973292, 2019.
- [20] T. I. Fossen, *Mathematical Models for Control of Aircraft and Satellites*, 2nd Edition, Department of Engineering Cybernetics, Norwegian University of Science and Technology, Norway, 2011.
- [21] G. Nugroho and A. Dharmawan, Undesirable rolling minimization on the EDF missiles flight based on LQR methods, *2017 International Conference on Advanced Mechatronics, Intelligent Manufacture, and Industrial Automation (ICAMIMIA)*, doi: 10.1109/ICAMIMIA.2017.8387563, 2018.
- [22] K. Ogata, *Modern Control Engineering*, 5th Edition, Prentice-Hall, New Jersey, USA, 2010.
- [23] F. Rinaldi, S. Chiesa and F. Quagliotti, Linear quadratic control for quadrotors UAVs dynamics and formation flight, *J. Intell. Robot. Syst.*, vol.70, nos.1-4, pp.203-220, doi: 10.1007/s10846-012-9708-3, 2012.